ASEAN Engineering Journal

Full Paper

STRESS ANALYSIS OF TEETH, PERIODONTAL TISSUES, AND MAXILLA BONES DUE TO BRUXISM

Satrio Wicaksono[a], Andi Isra Mahyuddin[a], Aldilla Miranda[b], Tatacipta Dirgantara[a]*, Nunung Rusminah[b]

[a]Faculty of Mechanical and Aerospace Engineering, Institut Teknologi Bandung, Bandung, Indonesia
[b]Periodontology Department, Faculty of Dentistry, Universitas Padjadjaran, Bandung, Indonesia

Article history
Received
29 September 2021
Received in revised form
08 February 2022
Accepted
09 February 2022
Published online
30 November 2022

*Corresponding author
tdirgantara@ftmd.itb.ac.id

Graphical abstract

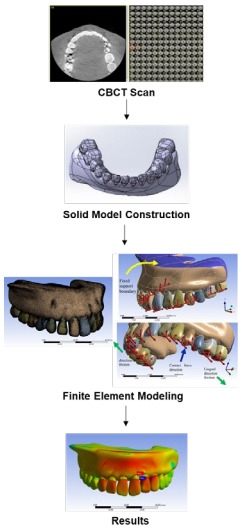

Abstract

This paper investigates the stress distribution on the teeth and jaw during bruxism that may provide additional insights to the consequences of bruxism, splint design considerations, a basis for possible therapy protocols, and a baseline for future bruxism studies. A three-dimensional (3D) solid model of a complete jaw comprised of teeth, periodontal ligaments, and maxilla bone is reconstructed based on a Cone Beam Computed Tomography (CBCT) scan of a patient. A finite element model of the jaw is then constructed using the geometry imported from the solid model that has been reworked to remove imperfections during reconstruction and to allow proper contact between teeth. A linear elastic finite element analyses were then performed to simulate the bruxism phenomenon which includes biting and grinding. Numerical analysis is conducted only to the maxilla, with forces are placed on the teeth's surface where contact occurs. The analysis is conducted for all stages of bruxism and possible movements patterns. Results suggest that high stresses occur during grinding, indicating a strong correlation between bruxism and dental issues such as tooth wear and alveolar resorption.

Keywords: Bruxism modeling, 3D reconstruction and modeling of jaw, Finite element analysis, Stress analysis

1.0 INTRODUCTION

Bruxism is a parafunctional habit consisting of clenching, grinding, and gnashing of the teeth. It is commonly described as a collection of several oral habitual abnormality primarily involving increase of muscle jaw activity resulting to lateral excursion of the mandible. About 8-34% of the general population may have bruxism with more prevalence to people under the age of 40 years old [1]. Furthermore, approximately 45 million people in the United States have a form of parafunctional habit such as bruxism. This activity in the long term may lead to several adverse effects including but not limited to tooth attrition, widening of the periodontal membrane, alveolar bone resorption, and even disruption of temporomandibular joint [2]. Additionally, Sugimoto, et al [3] discovered that extreme biomechanical loads from bruxism may cause further damage in terms of abfraction, hypersensitivity, periodontal distraction, muscle fatigue, and other dental issues. Bruxism is characteristically associated with complaints of awakening from sleep with dull or vise-like head pain, "looseness" of the jaw when articulated, and worn or fractured tooth enamel surfaces with concomitant exposure of dentin [4]. Bruxism usually occurs without any self-awareness and its causes is generalized into three factors which are peripheral, psychosocial, and pathophysiology factor [5-9].

To the knowledge of the authors, most available numerical simulation research relating to bruxism are mostly focused on studying the effects of bruxism to the stress distribution on the temporomandibular joint, such as that shown in Barrientos, et al [10] and Del Palomar and Doblare, et al [11]. Others available studies also commonly involves finite element analysis of dental implants as shown by Zhang, et al [12] and Marcián, et al [13]. Bălăcel, et al [14] investigated tooth wear relating to bruxism using finite element analysis and concluded that bruxism may produce wear pattern characteristic of attrition on occluding tooth surfaces. Larson [15] also investigated bruxism

movement pattern, bite force, and stress analysis on a single tooth. Recently, Budiaman, et al [16] presented a preliminary work on numerical analysis for stress distribution of teeth and periodontal tissues due to bruxism.

However, there has not been any further investigation regarding stress distribution due to traumatic occlusion by bruxism movement. The purpose of this paper is to investigate the stress distribution occurring around the teeth during bruxism. It is important to understand this stress distribution because it may provide dentists/researchers additional insights to consequences of bruxism on the teeth (e.g., wearing, abfraction, or attrition) and the jawbone (e.g., alveolar ridge resorption). The stress distribution may also aid dentists to determine certain splint designs that could mitigate prolonged clenching resulted by bruxism that may occur voluntarily or involuntarily. In this study, a more extensive work is presented, including the reconstruction of geometrical model of a human jaw, which has now become more accurate and simpler with a Cone Beam Computerized Tomography (CBCT) radiograph, and a complete finite element analysis of the modeled jaw. This research utilizes a 3D solid model of the mouth using finite element method to predict the stress distribution resulted from bruxism.

2.0 MATERIALS AND METHODS

2.1 CAD for the teeth, Periodontal Ligaments, and Maxilla

The analysis for this research requires the solid model of the maxillary teeth, their periodontal ligaments, and the maxilla. The computer models for these body parts are based on a patient experiencing bruxism. The maxillary teeth and maxilla bone were both obtained with similar procedure described as follow. First, the patient's teeth are scanned using a CBCT radiograph, the machine used was KaVo OP 3DTM. These scan results were in the form of slices of cross section of the object. Figure 1a shows an example of scan results for the teeth. These scans were used to generate a cloud point representation of the patient's teeth using 3D-Doctor ®. The point cloud for both teeth and maxilla were generated by means of defining a region of interest and the boundary area that outlines the teeth or the maxilla for each slice of scanned cross-section. For instance, the outline shown in Figure 1b shows the region of interest which indicate a high probability of where the object of interest (e.g., the teeth) was located. The boundary area which indicates the cross-section image of the object of interest on one scan is identified automatically within the region of interest by thresholding. The shades shown in Figure 1b is the boundary area of teeth identified by the thresholding method. Finally, the 3D point cloud model was used to generate the 3D solid CAD model using SOLIDWORKS 2020®. These processes are cleaning, smoothing, and auto surface reconstruction. The two former processes were used to clear several imperfections of the model to prevent misrepresenting sharp edges that would appear as stress concentrations in the finite element analysis. Figure 2a shows the result of the cleaning and smoothing process. The auto surface reconstruction process was used to generate a surface of the model based on the preprocessed point cloud data (Figure 2b) which was later used to generate a solid model. The teeth were formed into a solid model from the surfaces by the "closed surface" operation. Figure 2c shows an example of a resulting solid 3D model of a single tooth. The same steps were applied to create a solid model for the maxilla (Figure 2d). The tooth socket for the maxilla was added in a later process. Additionally, Table 1 shows the overall dimension of the subject's maxilla and Table 2 shows the overall dimension of the subject's teeth.

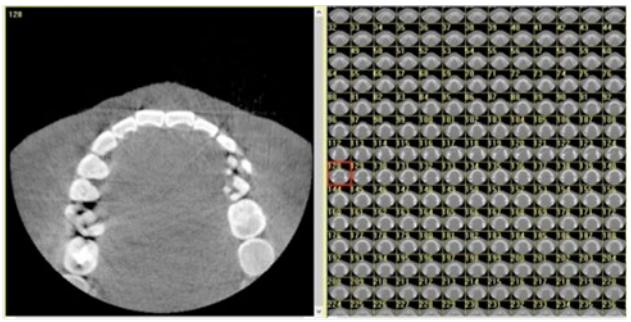

(a)

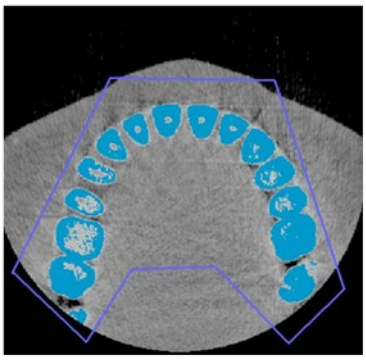

(c)

Figure 1 CBCT scan result and its preprocessing steps: (a) Cross sections of the upper jaw; (b) Example of the boundary area for the maxillary teeth within the region of interest

The steps to produce the periodontal ligament was different than the teeth and the maxilla. Since the periodontal ligament surrounds nearly all the root portion of the tooth, its 3D model is essentially a solid model generated by forming a new body from the surface of the teeth's root portion and extruding the surface outward with a 0.1 mm thickness as shown in Figure 2e. Figure 2f shows the fully assembled model for the finite element analysis. Each of the tooth, maxilla, and periodontal ligament has a certain coordinate location with respect to a common origin which makes it easy for the software to position them accordingly as a full maxilla assembly using the "Boolean" operation. This operation not only positions the components accordingly, but also create intersections to the maxilla, forming the tooth socket. This final operation completes the geometric modelling for the maxilla (Figure 2g).

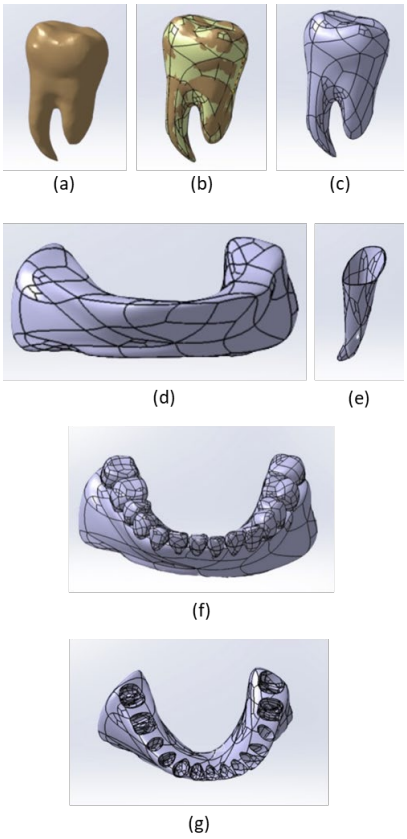

Figure 2 Construction steps of 3D solid model and their results: (a) Cleaning and smoothing operation result for 3D point cloud of a tooth; (b) Generating 3D surface on the 3D point cloud; (c) 3D solid model generated using closed surface operation; (d) Resulting solid 3D model for the maxilla; (e) Resulting solid 3D model for a Periodontal Ligament; (f) Final full assembly for the maxilla; (g) Resulting complete solid model for the maxilla

Table 1 Maxilla dimension

Measured Dimension	Value (mm)
Incisor-canine distance (ICD)	6
Incisor-1st molar distance (IM1D)	23
Incisor-2nd molar distance (IM2D)	36
Intercanine distance (CW)	36
1st molar width (M1W)	56
2nd molar width (M2W)	60

Table 2 Teeth dimension

Measured Dimension	Mediodistal (mm)	Cervico-occlusal (mm)	Buccolingal (mm)
Incisor	7.5	10.5	3.5
Canine	6	10	5
Premolar	6	7	8.5
Molar	9	6	10.5

2.2 Finite Element Model

The maxilla, periodontal ligament, and teeth material properties was applied to their respective models by simply assigning their respective material's tensile strength, compressive strength, modulus of elasticity, and Poisson's ratio values to the finite element model settings. The maxilla uses two material properties which are the trabecular bone and the cortical bone similar to a real maxilla structure while the teeth are fully modeled using dentin material. These material assignments to the simulation models follow the same approach as the research conducted by Ekachai as shown in Table 3 [17] with addition to the material's strength [18, 19]. Using the obtained 3D solid model, the mesh model was generated automatically by the analysis software (ANSYS 2020R2®) using tetrahedron elements. The validity of the mesh model was observed by comparing the maximum stress of a certain point within the model and the number of elements produced by the meshing model. The mesh model is valid if the stress levels converge to a certain value as the number of elements increase. The convergence plot (Figure 3) shows that the finite element model should give out valid results if the number of elements exceeds at least two million. The final finite element model in this study (Figure 4) uses 2,653,550 elements, with smallest size at 46 µm and biggest size at 9.2 mm. Homogenous and isotropic material properties was assumed while the contact between components was assumed as bonded.

Table 3 Material properties

Material	Modulus of Elasticity (MPa)	Poisson's Ratio	Tensile Strength (MPa)	Compressive Strength (MPa)
Cortical Bone	14500	0.323	133	205
Trabecular Bone	1370	0.300	121	170
Periodontal Ligament	50	0.490	52	75
Tooth (Dentin)	18600	0.350	98	400

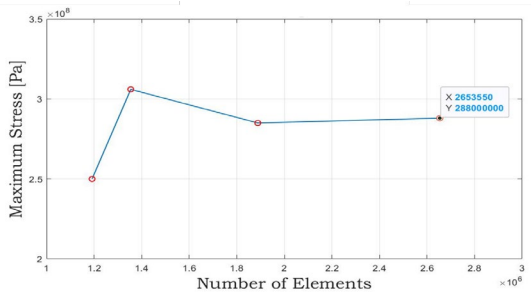

Figure 3 Mesh convergence plot

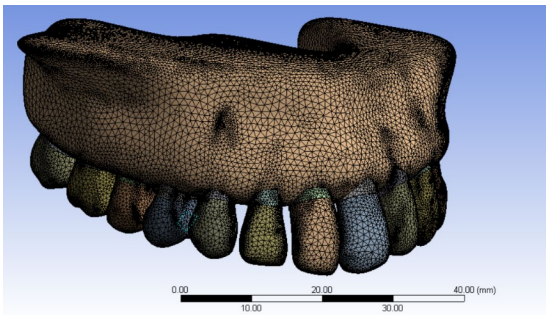

Figure 4 Meshing model of the maxilla assembly

2.3 Modeling Bruxism Phenomena

In modeling bruxism, two types of loads were defined on the teeth during bruxism which are contact and grinding forces. The contact force was represented with a force applied on the long axis of a tooth which tends to point in the positive z-axis (Figure 5). The load from grinding was applied perpendicularly to the contact force which tends to point in the y-axis. The load given in the simulation is static load. During grinding, the grinding force's direction alternates between the positive and negative side of the y-axis. Fixed support was defined on the top surface of the maxilla model (Figure 5). In this research, bruxism was modeled based on its load cases and how these loads are applied to different areas of the teeth based on five different movements.

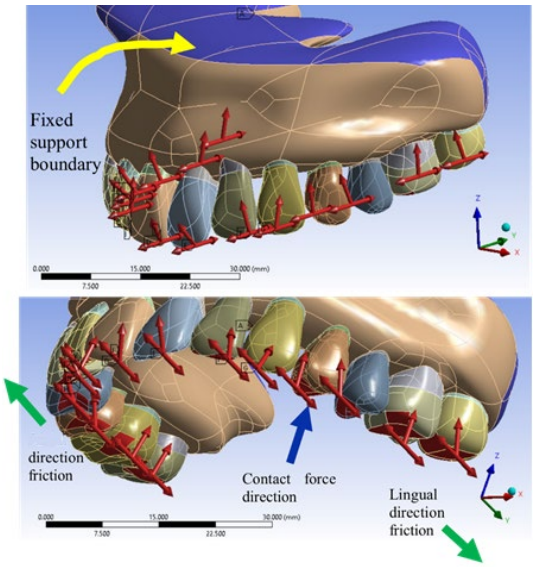

Figure 5 Loading condition to the teeth and the fixed support

There are three load cases occurring sequentially during bruxism. Hence, the simulation is divided into three steps based on these load cases which are the initial contact load, friction toward lingual direction, and friction toward buccal direction. Both lingual and buccal direction friction movement was considered as the grinding forces while the initial contact load was a contact force. During initial contact, the incisor and canine teeth receive an impact force of 569 N while the molars receive 911 N. This is considerably higher than regular mastication which is about 90 to 180 N. After initial contact, the contact force between the upper and lower teeth decreased and remains in 200 N throughout the succeeding steps. The second step is the friction towards lingual direction where the force points towards the positive y-axis (Figure 5). The third step is the friction towards the buccal direction pointing to the negative y-axis. Both friction's magnitude was set to be 200 N [15]. Note that the primary distinction between bruxism and functional mastication lies on the initial contact force and the duration of the activity where bruxism has higher initial contact force and longer duration.

What makes bruxism also discernable from regular mastication is how these forces are applied to the teeth. During sleep bruxism, there are two types of grinding movement which affects how the load is applied to the teeth: the Laterotrusive-side and Mediotrusive-side movement patterns. The Laterotrusive-side is the facet of the tooth that faces the lingual direction. The Mediotrusive-side is the facet of the tooth at the slope of a molar tooth up to its palatal peak. Laterotrusive-side movements have three subcategories which are the incisor-canine (IC), incisor-canine-premolar (ICP), and incisor-canine-premolar-molar (ICPM) grinding movement. The Mediotrusive-side movement is divided into two more subcategories which are the Mediotrusive Contact (MC) and Mediotrusive Grinding (MG) [3, 20]. This means that, for every load case mentioned, there are five different contact-area cases that may occur at any time during bruxism. Figure 6a illustrates the loading condition on the teeth during the Laterotrusive-side movement patterns for the IC case where force is applied to the lingual side of the incisor and canine teeth. Figure 6b and c illustrates the loading condition during ICP and ICPM, respectively. Figure 7a illustrates the loading condition of the teeth during the MC case where force is applied on a small area on the premolar and molar teeth. Figure 7b illustrates the MG case where the contact area is in a wider area over all the molar teeth. All five of these alternative contact-area cases were applied to the model.

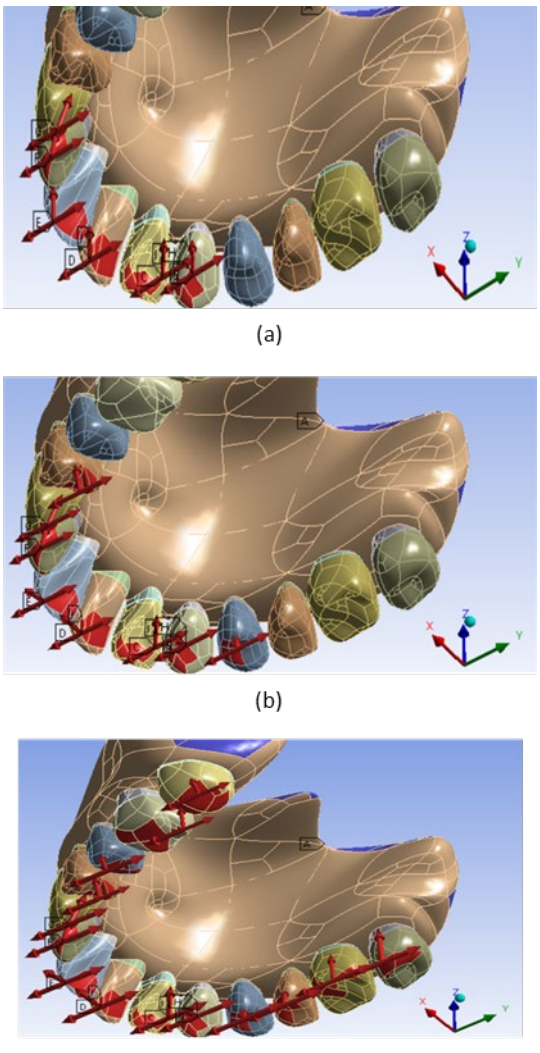

Figure 6 Laterotrusive-side movements: (a) The Incisor-Canine; (b) Incisor-Canine-Premolar; (c) Incisor-Canine-Premolar-Molar

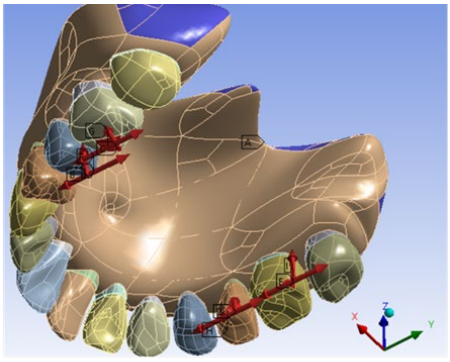

(a)

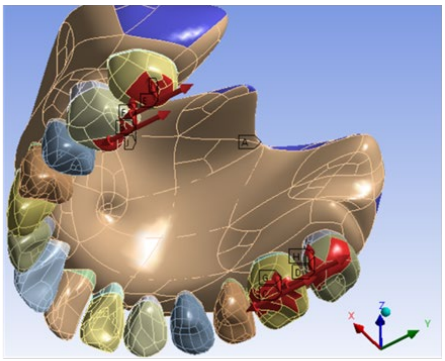

(b)

Figure 7 Mediotrusive-side movements: (a) Mediotrusive contact; (b) Mediotrusive grinding

3.0 RESULTS

Evaluation of the maxilla assembly during bruxism loading is focused on three key events: during initial contact of the teeth, grinding movement in the lingual direction, and the grinding movement in the buccal direction. Principal stresses occurring at the teeth, maxilla, and periodontal ligament is compared to the tensile and compressive strength of the respective materials. The reason this research chooses to evaluate principal stress is because all the materials that make up the assembly are considered brittle. Thus, it would be convenient to compare the principal stress occurring at the maxilla assembly with the strength of each brittle component in the sense of the failure of brittle materials. Table 4 to Table 6 presents the resulting principal stresses during initial contact, lingual direction grinding, and buccal direction grinding, respectively. Each table shows the stresses during each five contact-area cases. Attention is made to the resulting principal stresses that exceeds the tensile and compressive strengths of the occurring material. Figure 8 to Figure 12 shows the location of the maximum principal stresses on the maxilla assembly during the five contact-area cases of IC, ICP, ICPM, MC, and MG, respectively.

Table 4 Principal stress value due to contact force from initial contact movement

Contact Area	Teeth		Periodontal Ligament		Alveolar Bones	
	Principal Stress Value (MPa)					
	T	C	T	C	T	C
IC (incisor-canine)	26	62	33	34	100	130
ICP (incisor-canine-premolar)	87	85	62	43	229	166
ICPM (incisor-canine-premolar-molar)	87	85	62	43	230	172
MC (mediotrusive contact)	67	168	15	23	44	37
MG (mediotrusive grinding)	15	16	8	15	16	20

T = Tension
C = Compression

Table 5 Principal stress value due to friction from grinding movement toward the lingual direction

Contact Area	Teeth		Periodontal Ligament		Alveolar Bones	
	Principal Stress Value (MPa)					
	T	C	T	C	T	C
IC (incisor-canine)	156	151	47	119	285	280
ICP (incisor-canine-premolar)	156	151	55	116	291	286
ICPM (incisor-canine-premolar-molar)	156	150	59	114	295	290
MC (mediotrusive contact)	206	32	64	69	118	146
MG (mediotrusive grinding)	35	50	38	34	59	68

T = Tension
C = Compression

Table 6 Principal stress value on due to friction from grinding movement toward the buccal direction

Contact Area	Teeth		Periodontal Ligament		Alveolar Bones	
	Principal Stress Value (MPa)					
	T	C	T	C	T	C
IC (incisor-canine)	151	156	119	47	285	288
ICP (incisor-canine-premolar)	150	156	110	55	284	294
ICPM (incisor-canine-premolar-molar)	150	155	109	59	288	298
MC (mediotrusive contact)	132	206	50	64	146	118
MG (mediotrusive grinding)	50	35	34	37	68	59

T = Tension
C = Compression

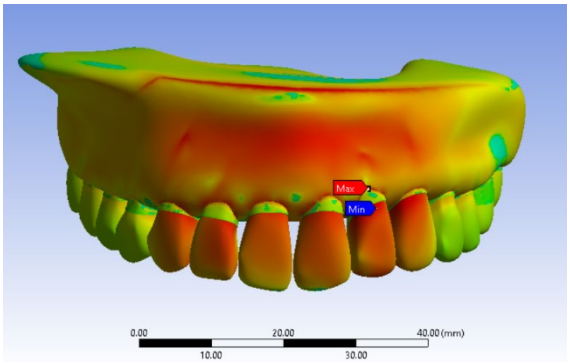

Figure 8 Principal stresses during IC movement

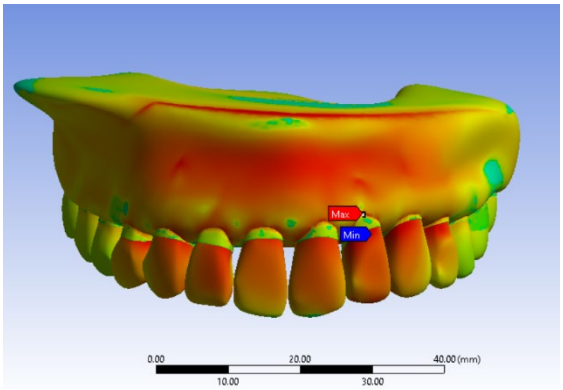

Figure 9 Principal stresses during ICP movement

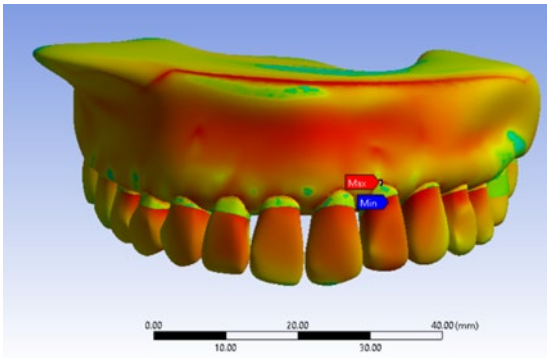

Figure 10 Principal stresses during ICPM movement

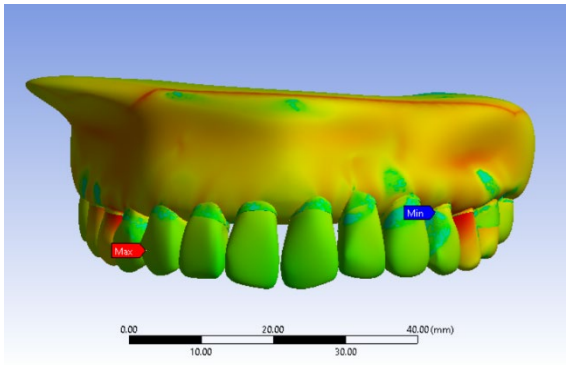

Figure 11 Principal stresses during MC movement

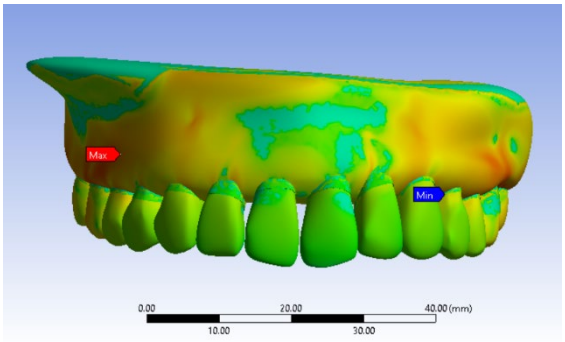

Figure 11 Principal stresses during MG movement

4.0 DISCUSSIONS

Tables 4 to 6 show that the friction resulted from the grinding movement causes more stress on the maxilla assembly than the contact force from the initial contact movement despite such high loads at the initial stages of bruxism (underlined values mean that it exceeds the ultimate strength of the component). The teeth itself does not seem to suffer a lot from the high forces (569 N on the incisor and canine and 911 N on the premolar and molar teeth) during first contact of the teeth. However, Table 5 and 6 shows that the teeth receive tremendous principal stresses during grinding as these stresses exceeds the teeth's tensile strength (98 MPa). The highest stress value on the teeth is 206 MPa during the contact-area resulted from the Mediotrusive-contact during grinding at the lingual direction, which is more than twice the tensile strength of the teeth's material. An important note is that during both grinding directions (Table 5 and 6), stresses at the teeth in nearly all contact-area cases exceed the material's strength. This may explain why most of the adverse effects on the teeth such as tooth wear reported from bruxism may primarily came from prolonged involuntary grinding movement of the mouth. Additionally, high stresses are also dominant at the alveolar bone of the maxilla. These high stresses across many cases of contact area during both grinding movements on the maxilla bone may be responsible for cases of alveolar ridge resorption. The highest stress occurring at the maxilla bone is 298 MPa at ICPM contact during grinding movement toward buccal direction which is nearly 50% larger than the material's compressive strength. In fact, the alveolar bones suffer the most during all the Laterotrusive-side movement while the teeth suffer stresses during both the Laterotrusive and Mediotrusive-side movement. Even though there are several cases to which the periodontal ligaments receive stresses exceeding its assigned material strength, damage to the periodontal ligament only occurs when there is damage to both teeth and maxilla bone since the periodontal ligament's function is similar to a "shock breaker" during mastication due to its ability to absorb occlusal forces to protect vessels, nerves, and bone from injury [21]. Nonetheless, it is important to note how much stress the periodontal ligament is receiving relative to other parts of the jaw assembly. It may be observed that the jaw assembly is much more impacted during grinding movement rather than the initial contact movement. High stresses occur more often during grinding in nearly all of contact-area types. It is possible that bruxism therapy should

give special attention to the grinding movement as more damage are likely due to this stage, although this decision should be left to the therapists.

5.0 CONCLUSION

In this work, an in-silico analysis using finite element has been conducted to obtain stresses at the teeth, periodontal ligament, and maxilla bones. The first important step prior to the finite element analysis is to obtain an accurate geometry which is based on a real patient. Data of the patient's teeth model is obtained using CBTB radiograph and the data is further processed using various tools to create a final 3D solid model of the whole maxilla assembly adequate for the finite element analysis. The validity of the meshing for the analysis is also verified by mesh convergence.

Results shown an overall conclusion that damage to the maxilla assembly, notably for both the teeth and jaw, is highly due to the high stresses occurring dominantly during grinding in either direction instead of the initial contact between teeth which is known to have a very high impact force. The dominantly occurring maximum stresses at the alveolar bones and the teeth during grinding may be the main cause of reported alveolar resorption. The high stresses exceeding tensile strength of the teeth during grinding movement may also add to the explanation to why teeth wearing is correlated to bruxism. It is hopeful that this study may add significant insights to dentists in terms of understanding how bruxism damages oral health. Hopefully, this research may initiate further study in terms of how bruxism causes damage which may also lead to research on designing the appropriate splint designs and potentially accurate therapy procedures for bruxism patient.

Acknowledgement

The authors acknowledge the research funding provided by The Ministry of Research and Technology/National Research and Innovation Agency of Indonesia under the grant of Penelitian Dasar Unggulan Perguruan Tinggi (PDUPT) as well as Institut Teknologi Bandung under the grant of Program Penelitian, Pengabdian kepada Masyarakat dan Inovasi (P3MI). The authors also acknowledge Nandy Achmad Fauzy, Edgar Sutawika, Anthony Sugiharta Budiaman, and Muhammad Yusril Sulaiman for the assistance in this research article.

References

[1] von Piekartz, H., Rösner, C., Batz, A., Hall, T., and Ballenberger, N. 2020. Bruxism, temporomandibular dysfunction and cervical impairments in females–Results from an observational study. *Musculoskeletal Science and Practice*. 45: 102073. DOI: https://doi.org/10.1016/j.msksp.2019.102073

[2] Rupprecht R. 2004. Trauma from occlusion: a review. *Clinical Update*. 26: 3

[3] Sugimoto, K., Yoshimi, H., Sasaguri, K., and Sato, S. 2011. Occlusion factors influencing the magnitude of sleep bruxism activity. *CRANIO®*. 29(2): 127-137. DOI: https://doi.org/10.1179/crn.2011.021

[4] Hathaway, K. M. 1995. Bruxism: definition, measurement, and treatment. *Advance in pain research and therapy*. 21: 375-386.

[5] Komiyama, O., Lobbezoo, F., De Laat, A., Iida, T., Kitagawa, T., Murakami, H., Kato, K., and Kawara, M. 2012. Clinical management of implant prostheses in patients with bruxism. *International Journal Of Biomaterials*. DOI: https://doi.org/10.1155/2012/369063

[6] Gümüş, H. Ö., Kılınç, H. İ., Tuna, S. H., and Özcan, N. 2013. Computerized analysis of occlusal contacts in bruxism patients treated with occlusal splint therapy. *The journal of advanced prosthodontics*. 5(3): 256-261. DOI: https://doi.org/10.4047/jap.2013.5.3.256

[7] Johansson, A., Omar, R., and Carlsson, G. E. 2011. Bruxism and prosthetic treatment: a critical review. *Journal of prosthodontic research.* 55(3): 127-136. DOI: https://doi.org/10.1016/j.jpor.2011.02.004

[8] Shetty, S., Pitti, V., Satish Babu, C. L., Surendra Kumar, G. P., and Deepthi, B. C. 2010. Bruxism: a literature review. *The Journal of Indian Prosthodontic Society*. 10(3): 141-148. DOI: https://doi.org/10.1007/s13191-011-0041-5

[9] Bender, S. D. 2009. Occlusion, Function, and Parafunction: Understanding the Dynamics of a Healthy Stomatagnathic System. *ADA CERP*.

[10] Barrientos, E., Pelayo, F., Tanaka, E., Lamela-Rey, M. J., Fernández-Canteli, A., and de Vicente, J. C. 2020. Effects of loading direction in prolonged clenching on stress distribution in the temporomandibular joint. *Journal of the Mechanical Behavior of Biomedical Materials*. 112: 104029. DOI: https://doi.org/10.1016/j.jmbbm.2020.104029

[11] Del Palomar, A. P., and Doblare, M. 2006. Finite element analysis of the temporomandibular joint during lateral excursions of the mandible. *Journal of biomechanics*. 39(12): 2153-2163. DOI: https://doi.org/10.1016/j.jbiomech.2005.06.020

[12] Zhang, L., Wang, Z., Chen, J., Zhou, W., and Zhang, S. 2010. Probabilistic fatigue analysis of all-ceramic crowns based on the finite element method. *Journal of biomechanics*. 43(12): 2321-2326. DOI: https://doi.org/10.1016/j.jbiomech.2010.04.030

[13] Marcián, P., Borák, L., Valášek, J., Kaiser, J., Florian, Z., and Wolff, J. 2014. Finite element analysis of dental implant loading on atrophic and non-atrophic cancellous and cortical mandibular bone–a feasibility study. *Journal of biomechanics*. 47(16): 3830-3836. DOI: https://doi.org/10.1016/j.jbiomech.2014.10.019

[14] Bălăcel, E., Lăcătuşu, Ş., Topoliceanu, C., Bălăcel, I., Iovan, G., and Ghiorghe, A. 2011. Mathematics model analysis of biomechanical behaviour of three dental materials to loading related to bruxism. *Romanian Journal of Oral Rehabilitation*. 3(3): 26.

[15] Larson, T. D. 2012. The effect of occlusal forces on restorations. *Northwest Dentistry*. 91(6): 25-7.

[16] Budiaman, A. S., Dirgantara, T., Miranda, A., Mihradi, S., and Mahyuddin, A. I. 2015, September. Numerical Analysis on Stress Distribution of Teeth and Periodontal Tissues due to Bruxism (GS1: Cell and Tissue Biomechanics VI). In *The Proceedings Of The Asian Pacific Conference On Biomechanics: Emerging Science And Technology In Biomechanics.* 139. DOI: https://doi.org/10.1299/jsmeapbio.2015.8.139

[17] Chaichanasiri, M., Nanakorn, P., and Tharanon, W. (2009). Finite element analysis of bone around a dental implant supporting a crown with a premature contact. *J Med Assoc Thai*. 92(10): 1336-44.

[18] Sharmila, H. 2004. Textbook of dental materials. India: Gopsons Paper Ltd Noida.

[19] Black, J., and Hastings, G. 2013. Handbook of biomaterial properties. Springer Science & Business Media.

[20] Wijaya, Y., Himawan, L. S., and Odang, R. W. 2013. Occlusal grinding pattern during sleep bruxism and temporomandibular disorder. *Journal of Dentistry Indonesia*. 20(2): 25-31.

[21] Dean, R. 2017. The periodontal ligament: development, anatomy and function. *Oral Health Dental Management*. 16(6): 1-7